A multiphase material model considering strain-induced crystallisation in polymers

K. Loos, A. Lion & M. Johlitz
Institute of Mechanics, Faculty for Aerospace Engineering, Universität der Bundeswehr Munich, Germany

J. Calipel
MICHELIN Technology Center, Clermont-Ferrand, France

ABSTRACT: The crystallisation ability of polymers under high stretches is a challenging phenomenon in material science. Multiphase approaches help scientists to distinguish between different structures, which evolve or vanish during experimental studies. Here, the observed phenomenon is the evolution of crystals during a uniaxial tensile test.

The current paper introduces an approach considering three different phases in one fibre of polymer. The free energy of the material considers the contribution of the mixing entropy. The derivation of the mixing entropy is explained in detail, making use of different assumptions and approaches, e.g. consideration of ideal mixtures.

In the end, this multiphase approach for the free energy is implemented in a constitutive model for rubbery materials stretched to high strains. It is able to depict the strain-induced crystallisation phenomenon observed via a uniaxial tensile test, prooved by stress-stretch and crystallinity-stretch simulations.

1 INTRODUCTION

The modelling of material behaviour plays an important role in industrial applications. Experiments, continuum mechanics and numerics are necessary to develop a mathematical model in order to understand and predict material behaviour. The observed polymer is an unfilled, vulcanized crystallisable natural rubber (NR).

The overall objective is to develop constitutive equations which reproduce its material behaviour. Focus is the stress-strain response including mechanical hysteresis which occurs for example during a uniaxial tensile test. The phenomenon of strain induced crystallisation (SIC) is the main hysteresis source for unfilled natural rubber during loading-unloading cycles. For the filled rubber, Mullins and viscous effects are also to be considered as other hysteresis sources.

The model uses a multiphase approach, i.e. one rubber fibre includes three different contributions: a crystalline phase and an amorphous phase which is compounded by a crystallisable amorphous part and a non-crystallisable amorphous part. Thus, different approaches for hyperelastic material models for each part are used for the formulation of the stress and the strain energy equations, which are an essential part of the first order differential equation of crystallinity.

The model is based on an additive split of the hybrid free energy into a Gibbs-type contribution representing the volumetric part and a Helmholtz contribution representing the isochoric part (Lion, Dippel, & Liebl 2014) and (Guilie, Le, & Le Tallec 2015). The isochoric free energy includes the free energies of the single phases and one part derived from a mixing entropy contribution, which is focus of the current paper.

The constitutive equations are physically and chemically motivated. The constitutive equations ensure thermodynamic consistency.

2 THE PHENOMENON OF STRAIN-INDUCED CRYSTALLISATION IN NATURAL RUBBER

In several industrial applications, natural rubber is essential due to its advantageous tensile properties. A fundamental characteristic of natural rubber is its ability to develop directional anisotropies when highly stretched in one direction $\vec{e}_\alpha$. This phenomenon is called strain-induced crystallisation and was first discovered by Katz (1925) via x-ray scattering.

2.1 *Directional crystallinity in a fibre of polymer*

In this framework, the fundamental idea modelling strain-induced crystallisation in NR, is to divide the total mass of the fibre m_α into two phases. First, the material has a crystalline phase with its mass $m_{\alpha c}$, which evolves at high stretches. Second, the
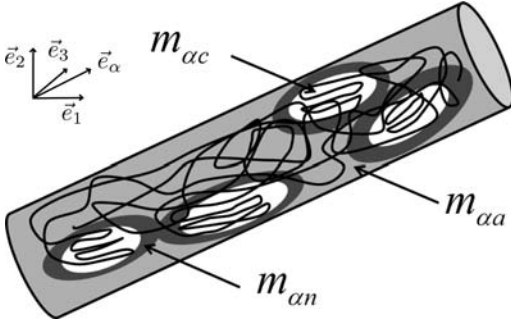
Figure 1. Phases in one fibre of elastomer: the crystallisable amorphous $m_{\alpha a}$, the non-crystallisable amorphous $m_{\alpha n}$ and the crystalline phase $m_{\alpha c}$, (Loos, Johlitz, Lion, Palgen, & Calipel 2017).

material has an amorphous phase existing during all stretches, also in the unstretched state. The idea is, that the amorphous phase is subdivided into a crystallisable amorphous fraction $m_{\alpha a}$ and a non-crystallisable amorphous fraction $m_{\alpha n}$, i.e. the total mass forms to

$$m_\alpha = m_{\alpha c} + m_{\alpha a} + m_{\alpha n}. \tag{1}$$

The sketch in Figure 1 visualises the idea of three mass contributions. The directional crystallinity x_α in $\vec{e}_\alpha$-direction is defined by its mass fraction

$$x_\alpha = \frac{m_{\alpha c}}{m_\alpha}. \tag{2}$$

Next, it is assumed, that there exists a linear dependence between the non-crystallisable fraction and the crystalline phase, i.e. each crystalline part possesses or is surrounded by a non-crystallisable amorphous part: $m_{\alpha n} = \zeta m_{\alpha c} \Leftrightarrow \frac{m_{\alpha n}}{m_{\alpha c}} = \zeta$.

The straight forward calculation starting from (1) and using the above definitions shows that the crystallisable amorphous fraction can be expressed as

$$1 = \frac{m_{\alpha c}}{m_\alpha} + \frac{m_{\alpha a}}{m_\alpha} + \frac{m_{\alpha n}}{m_{\alpha c}}\frac{m_{\alpha c}}{m_\alpha}$$

$$\Leftrightarrow \quad 1 = x_\alpha + \frac{m_{\alpha a}}{m_\alpha} + \zeta x_\alpha$$

$$\Leftrightarrow \quad \frac{m_{\alpha a}}{m_\alpha} = 1 - (1+\zeta)x_\alpha. \tag{3}$$

Consequently, the maximum value of the crystallisable amorphous phase is physically limited to 100%, which results to the definition of a maximum crystallinity x_0:

$$0 \leq x_\alpha \leq \frac{1}{1+\zeta} =: x_0. \tag{4}$$

With these abbreviations, each mass fraction simplifies to

$$\frac{m_{\alpha c}}{m_\alpha} = x_\alpha, \qquad \text{(directional crystallinity)}$$

$$\frac{m_{\alpha a}}{m_\alpha} = 1 - \frac{x_\alpha}{x_0} \quad \text{and} \qquad \text{(cryst. amorphous frac.)}$$

$$\frac{m_{\alpha n}}{m_\alpha} = \frac{x_\alpha}{x_0} - x_\alpha. \qquad \text{(non-cryst. amorphous frac.)}$$

The specific[1] directional Helmholtz free energies of the single phases are stated as

$$\hat{\psi}_{\alpha a}(\hat{\lambda}_\alpha, \theta), \qquad \text{(cryst. amorphous phase)}$$

$$\hat{\psi}_{\alpha n}(\hat{\lambda}_\alpha, \theta), \qquad \text{(non-cryst. amorphous phase)}$$

$$\hat{\psi}_{\alpha c}(\hat{\lambda}_\alpha, \theta), \qquad \text{(crystalline phase)}$$

which are all considered to be stretch and temperature dependent.

The total Helmholtz free energy $\hat{\Psi}_\alpha$ includes the free energy of the individual phases

$$\hat{\Psi}_{\alpha 0} = m_{\alpha a}\hat{\psi}_{\alpha a} + m_{\alpha c}\hat{\psi}_{\alpha c} + m_{\alpha n}\hat{\psi}_{\alpha n} \tag{5}$$

and the entropy of mixing[2]

$$S_{\text{mix}} = -m_\alpha \frac{R}{M}\gamma(x_\alpha), \tag{6}$$

where R is the universal gas constant, M is the molar mass and the function $\gamma(x_\alpha)$ is the mixing ratio. This leads to the total Helmholtz free energy

$$\hat{\Psi}_\alpha = \hat{\Psi}_{\alpha 0} - \theta S_{\text{mix}}. \tag{7}$$

The directional Helmholtz free energy per unit mass follows as

$$\hat{\psi}_\alpha = \left(1 - \frac{x_\alpha}{x_0}\right)\hat{\psi}_{\alpha a} + x_\alpha\hat{\psi}_{\alpha c} + \left(\frac{x_\alpha}{x_0} - x_\alpha\right)\hat{\psi}_{\alpha n}$$

$$+ \frac{R\theta}{M}\gamma(x_\alpha). \tag{8}$$

2.2 Mixing entropy

The specific directional Helmholtz free energies of the single phases; $\hat{\psi}_{\alpha a}(\hat{\lambda}_\alpha, \theta)$ for the crystallisable amorphous phase, $\hat{\psi}_{\alpha c}(\hat{\lambda}_\alpha, \theta)$ for the crystalline phase and $\hat{\psi}_{\alpha n}(\hat{\lambda}_\alpha, \theta)$ for the non-crystallisable amorphous interphase, add to the first term in equation (7), which is the free energy of the individual phases

---

[1] The directional Helmholtz free energy per unit mass is defined as $\hat{\psi}_\alpha = \frac{\hat{\Psi}_\alpha}{m_\alpha}$.

[2] The wording 'entropy of mixing' or 'mixing entropy' is used as an abbreviation for the total change in the entropy of a mixture.

$\hat{\Psi}_{\alpha 0} = m_{\alpha a}\,\hat{\psi}_{\alpha a} + m_{\alpha c}\,\hat{\psi}_{\alpha c} + m_{\alpha n}\,\hat{\psi}_{\alpha n}$. The total directional Helmholtz free energy $\hat{\Psi}_\alpha$ in equation (7) contains a term including the entropy of the mixing S_{mix} which will be derived in the following subsection.

As a starting point, one considers ideal gases as material. The change in the inner energy U of a closed thermodynamic system is defined by the first law of thermodynamics

$$\mathrm{d}U = \delta Q + \delta W = \theta \mathrm{d}S - p\mathrm{d}V$$

$$\Leftrightarrow \delta Q = \mathrm{d}U + p\mathrm{d}V, \tag{9}$$

where δQ is the change in heat and δW is the change in work. In solid mechanics, the change in work is often split into two contributions, such as a change in pressure p or volume V and an isochoric change in work. For the ideal gas $\delta W = -p\mathrm{d}V$ holds. The change in heat is expressed as the change in entropy $\mathrm{d}S$ times temperature θ with the assumption of a reversible process.

For ideal gases, the thermal equation of state $pV = nR\theta$ and the caloric equation of state $U = nc_v\theta$ hold, where n is the amount of substance, R is the universal gas constant and c_v is the specific heat capacity at constant volume. Inserting these equations of state into equation (9), the change in heat forms to

$$\delta Q = nc_v\,\mathrm{d}\theta + \frac{nR\theta}{V}\mathrm{d}V. \tag{10}$$

Please note, that the change in heat is an inexact differential $\frac{\partial}{\partial\theta}\left(\frac{nR\theta}{V}\right) \neq \frac{\partial}{\partial V}(nc_v)$, because its effect on the state of the system can be compensated by the change in work δW. On the contrary, the change in entropy, i.e. $\mathrm{d}S = \frac{\delta Q}{\theta}$, is an exact differential when reversible conditions are assumed for the exchange, i.e. $\frac{\partial}{\partial\theta}\left(\frac{nR}{V}\right) = \frac{\partial}{\partial V}\left(\frac{nc_v}{\theta}\right)$. This results to the change in entropy

$$\mathrm{d}S = \frac{\delta Q}{\theta} = \frac{nc_v}{\theta}\,\mathrm{d}\theta + \frac{nR}{V}\mathrm{d}V \tag{11}$$

and the entropy after integration

$$S = nc_v\ln\left(\frac{\theta_2}{\theta_1}\right) + nR\ln\left(\frac{V_2}{V_1}\right) \tag{12}$$

for two different volumes V_1 and V_2 in which the same amount of ideal gas n is stored at different temperatures θ_1 and θ_2, sketched in Figure 2.

In order to find a formulation for the entropy of mixing, a mixing process under constant pressure and temperature is assumed, cf. (Müller 2013, p. 248), (Müller 1973, p.179–182). An ideal gas of volume V_A and amount of substance n_A is mixed with an ideal gas of volume V_B and amount of substance n_B. The initial state is shown on the left of Figure 3, where $pV_A = n_A R\theta$ and $pV_B = n_B R\theta$ hold. The mixture of volume $V_A + V_B$ and amount of substance $n_A + n_B$ is sketched on the right of
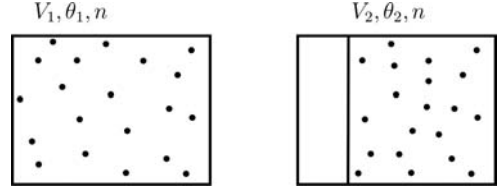

Figure 2. Sketch of two volumes V_1, V_2 with different temperatures θ_1, θ_2 and same number of particles n.
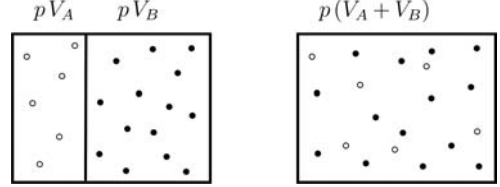

Figure 3. Sketch of the mixing process of two initial volumes V_A, V_B with different number of particles n_A, n_B of two ideal gases under constant hydrostatic pressure p and temperature θ.

Figure 3, where $p(V_A + V_B) = (n_A + n_B)R\theta$ holds. The respective changes in the entropies are

$$\Delta S_A = n_A R\ln\left(\frac{V_A + V_B}{V_A}\right) \quad \text{and} \tag{13}$$

$$\Delta S_B = n_B R\ln\left(\frac{V_A + V_B}{V_B}\right). \tag{14}$$

The total change in the entropy of the mixture is

$$S_{\mathrm{mix}} = \Delta S_A + \Delta S_B$$

$$= n_A R\ln\left(\frac{V_A + V_B}{V_A}\right) + n_B R\ln\left(\frac{V_A + V_B}{V_B}\right). \tag{15}$$

Note that the total volume is added up from the initial volumes $V = \sum_i V_i$, i.e. here $V_A + V_B$, only under consideration of ideal gases. In Müller (2013, p. 248ff) one can find a more general derivation of the mixing entropy, which is not assuming ideal gases. For ideal gases, the inner energy of the mixing is zero, i.e. $U_{\mathrm{mix}} = 0$ and the entropy of mixing is not equal to zero, i.e. $S_{\mathrm{mix}} \neq 0$, cf. (Müller 2013, p. 250f).

In this work, the possible inner energy of mixing is not taken into account such that the free energy of the mixing reads as $\Psi_{\mathrm{mix}} = U_{\mathrm{mix}} - \theta S_{\mathrm{mix}} \approx -\theta S_{\mathrm{mix}}$.

Now, the ideal gas equation is inserted into the volumes $V = \frac{nR\theta}{p}$, where temperature θ and pressure p remain constant within the assumption

$$S_{\mathrm{mix}} = n_A R\ln\left(\frac{n_A + n_B}{n_A}\right)$$

$$+ n_B R\ln\left(\frac{n_A + n_B}{n_B}\right). \tag{16}$$

Considering the Avogadro equation $n = \frac{N}{N_{\mathrm{Avo}}}$ on the one hand, where N_{Avo} is the Avogadro constant and N is

the number of constituent particles, and the definition of the amount of substance $n = \frac{m}{M}$ on the other hand, where m is the total mass and M is the molar mass of the substance, the mixing entropy results in

$$S_{\text{mix}} = \frac{m_A}{M_A} R \ln\left(\frac{N_A + N_B}{N_A}\right)$$

$$+ \frac{m_B}{M_B} R \ln\left(\frac{N_A + N_B}{N_B}\right). \tag{17}$$

This general example is now applied for the crystalline fibre, sketched in Figure 1. First, a crystalline particle is assumed to consist of the mass of the crystalline and that of the surrounding non-crystallisable amorphous material, i.e. $m_{\alpha\,\text{cryst}} = m_{\alpha c} + m_{\alpha n}$. In addition, all phases possess similar mean molar masses, i.e. $M = M_a = M_{\text{cryst}}$. With these considerations, the mixing entropy of a fibre with only two types of particles (crystalline particles + amorphous particles, i.e. $m_\alpha = m_{\alpha\,\text{cryst}} + m_{\alpha\,a}$) reads as

$$S_{\text{mix}} = \frac{m_{\alpha\,a}}{M_a} R \ln\left(\frac{N_{\alpha\,a} + N_{\alpha\,\text{cryst}}}{N_{\alpha\,a}}\right)$$

$$+ \frac{m_{\alpha\,\text{cryst}}}{M_{\text{cryst}}} R \ln\left(\frac{N_{\alpha\,a} + N_{\alpha\,\text{cryst}}}{N_{\alpha\,\text{cryst}}}\right). \tag{18}$$

Furthermore, the fractions of constituent particles can be expressed by fractions of crystallinities;

$$\frac{N_{\alpha\,a} + N_{\alpha\,\text{cryst}}}{N_{\alpha\,a}} = \frac{m_{\alpha\,a} + m_{\alpha\,\text{cryst}}}{m_{\alpha\,a}} = \frac{m_\alpha}{m_{\alpha\,a}} = \frac{x_0}{x_0 - x_\alpha}$$

$$\frac{N_{\alpha\,a} + N_{\alpha\,\text{cryst}}}{N_{\alpha\,\text{cryst}}} = \left(\frac{m_{\alpha n}}{m_\alpha} + \frac{m_{\alpha c}}{m_\alpha}\right)^{-1} = \frac{x_0}{x_\alpha}$$

refer to subsection 2.1 for the mass fractions of the different parts of one fibre.

The final expression reads as

$$S_{\text{mix}} = \frac{m_{\alpha\,a}}{M} R \ln\left(\frac{x_0}{x_0 - x_\alpha}\right) + \frac{m_{\alpha\,\text{cryst}}}{M} R \ln\left(\frac{x_0}{x_\alpha}\right)$$

$$= -m_\alpha \frac{R}{M}\left[\frac{x_0 - x_\alpha}{x_0} \ln\left(\frac{x_0 - x_\alpha}{x_0}\right) + \frac{x_\alpha}{x_0} \ln\left(\frac{x_\alpha}{x_0}\right)\right]$$

$$= -m_\alpha \frac{R}{M} \gamma(x_\alpha), \tag{19}$$

where

$$\gamma(x_\alpha) = \frac{x_0 - x_\alpha}{x_0} \ln\left(\frac{x_0 - x_\alpha}{x_0}\right) + \frac{x_\alpha}{x_0} \ln\left(\frac{x_\alpha}{x_0}\right) \tag{20}$$

is the mixing ratio of the fibre. Note that the mixing ratio has a maximum between $0 \leq x_{\text{max}} \leq x_0$, as shown in Figure 4.

For the evolution equation of crystallinity, equation (25), one needs the first derivative of the mixing ratio with respect to crystallinity:

$$\frac{d\gamma(x_\alpha)}{dx_\alpha} = \frac{1}{x_0} \ln\left(\frac{x_\alpha}{x_0 - x_\alpha}\right). \tag{21}$$
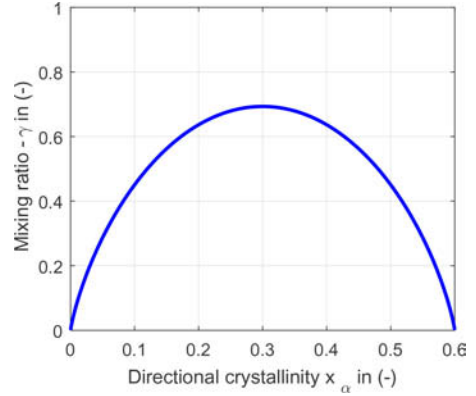

Figure 4.   Mixing ratio versus directional crystallinity with an exemplary maximum crystallinity of $x_0 = 0.6$.

Based on these considerations, the total specific directional Helmholtz free energy is defined as

$$\hat{\psi}_\alpha = \left(1 - \frac{x_\alpha}{x_0}\right)^n \hat{\psi}_{\alpha a} + x_\alpha^m \hat{\psi}_{\alpha c}$$

$$+ \left(\frac{x_\alpha}{x_0} - x_\alpha\right)^k \hat{\psi}_{\alpha n} + \frac{R\theta}{M} \gamma(x_\alpha), \tag{22}$$

where n, m and k are empirical exponents which emphasize the coupling between crystallinity and stress, explained in the next subsection. In equation (8), these exponents do not occur, but here they have been introduced to formulate a model with more flexibility to represent experimental data.

2.3   The evolution equation of the directional crystallinity

The expression of the mixing entropy is then used for the derivation of the evolution equation for the directional crystallinity which is directly achieved after the evaluation of the Clausius-Duhem inequality. The Clausius-Duhem inequality ensures the thermodynamical consistency of constitutive equations such that the second law of thermodynamics is satisfied:

$$-\rho_R \dot{\psi} + \tilde{\mathbf{T}} : \dot{\mathbf{E}} - \rho_R s \dot{\theta} - \frac{\vec{q}_R \cdot \vec{g}_R}{\theta} \geq 0, \tag{23}$$

where the state variables ρ_R, θ, ψ, s denote the density, the thermodynamic temperature, the specific Helmholtz free energy and the entropy per unit mass related to the reference configuration. $\mathbf{E}$ is the Green-Lagrange strain tensor, $\tilde{\mathbf{T}}$ is the second Piola-Kirchhoff stress, and $\tilde{\mathbf{T}} : \dot{\mathbf{E}}$ is consequently the stress power. Through the evaluation of the Clausius-Duhem inequality, the one dimensional evolution equation of the directional crystallinity is derived as

$$\dot{x}_\alpha = -\beta(\theta, ...)\left(\frac{\partial g}{\partial x} + \frac{\partial \hat{\psi}_\alpha}{\partial x_\alpha}\right), \tag{24}$$
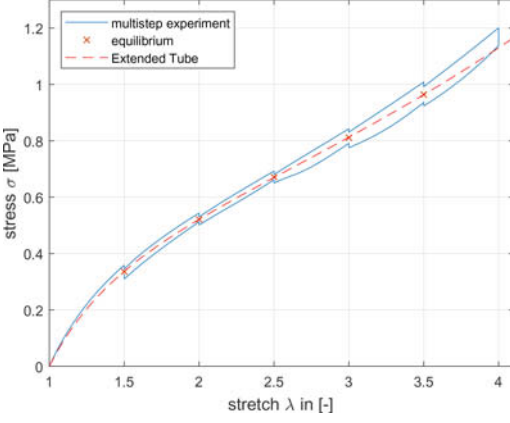
Figure 5. Multistep experiment at room temperature until stretch $\lambda_{max} = 3.5$ with equilibrium stresses marked with crosses and fitted extended tube hyperelastic model.
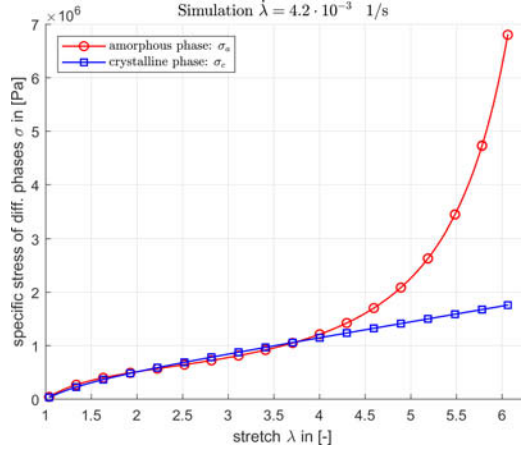

Figure 6. Stress response of single phases up to high stretch, using the neo-Hookean material model for the crystalline phase and the extended tube model for the amorphous phase.
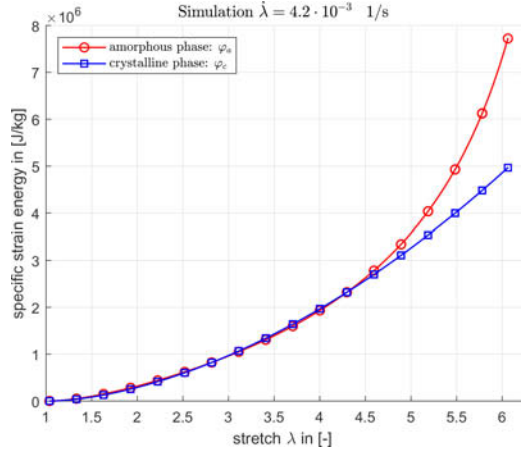

Figure 7. Strain energies of single phases up to high stretch, using the neo-Hookean material model for the crystalline phase and the extended tube model for the amorphous phase.

where $\beta(\theta, \dots)$ considers the temperature dependence of the material among other optional dependences on internal state variables. Temperature dependence is here represented by the approach by Williams, Landel, & Ferry (1955). Here holds, the higher the temperature, the less the evolution of the crystals.

Furthermore, a simplifying assumption considers, that the Gibbs-type energy contribution g, which represents the volumetric part of the material behaviour, does not depend on the total crystallinity x, therefore $\frac{\partial g}{\partial x} = 0$. The evolution equation of the directional crystallinity follows with the simplifying assumptions $\hat{\psi}_{\alpha a} = \hat{\psi}_{\alpha n}; n = k$ to

$$
\dot{x}_\alpha = -\beta \Bigg\{ \ \left[-\frac{n}{x_0}\left(1 - \frac{x_\alpha}{x_0}\right)^{n-1} \right.
$$

$$
+ n\left(\frac{1}{x_0} - 1\right)\left(\frac{x_\alpha}{x_0} - x_\alpha\right)^{n-1} \Bigg] \hat{\psi}_{\alpha a}
$$

$$
+ \ m\, x_\alpha^{m-1} \hat{\psi}_{\alpha c} - \frac{R\theta}{Mx_0} \ln\left(\frac{x_\alpha}{x_0 - x_\alpha}\right) \Bigg\}. \tag{25}
$$

The stress response of the single phases is derived through differentiation of the strain energy function with respect to stretch, i.e. $\sigma(\lambda) = \frac{\partial \psi(\lambda)}{\partial \lambda}$. With the above mentioned assumption, $\hat{\psi}_{\alpha a} = \hat{\psi}_{\alpha n}$, the total stress response is composed of the single stresses of the amorphous and the crystalline phase

$$
\sigma(\lambda, x_\alpha) = \left[\left(1 - \frac{x_\alpha}{x_0}\right)^n + \left(\frac{x_\alpha}{x_0} - x_\alpha\right)^n\right]\sigma_a(\lambda)
$$

$$
+ x_\alpha^m \sigma_c(\lambda). \tag{26}
$$

After evaluation of the main hyperelastic material models, the strain energy of the amorphous phase is modelled by the extended tube model proposed by Kaliske & Heinrich (1999) and the strain energy of the crystalline phase is modelled by the neo-Hookean material model as discussed in Treloar (1943). All model parameters (four for the extended tube and one for the neo-Hookean model) were found by fitting experimental data achieved through a multistep experiment, shown in Figure 5, in which unfilled natural rubber was stretched up to a low stretch of $\lambda = 3$ in order to avoid crystallisation, which occurs for the studied material at stretches above $\lambda = 4$.

The identified stresses of the single phases are shown in Figure 6 and the strain energies of the single phases are shown in Figure 7. The increasing gap between both phases implies the driving force for
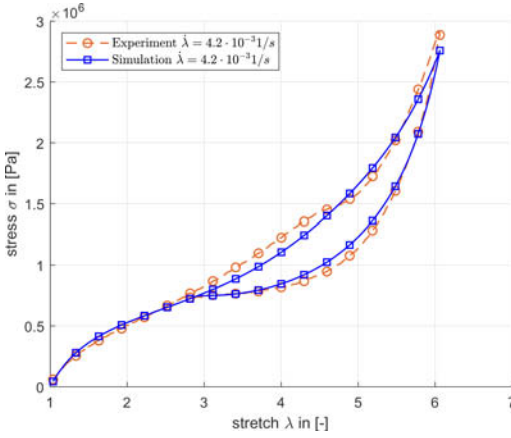
Figure 8. Stress over stretch of unfilled natural rubber, simulation vs. experiment at low strainrate, experimental data from Candau (2014).
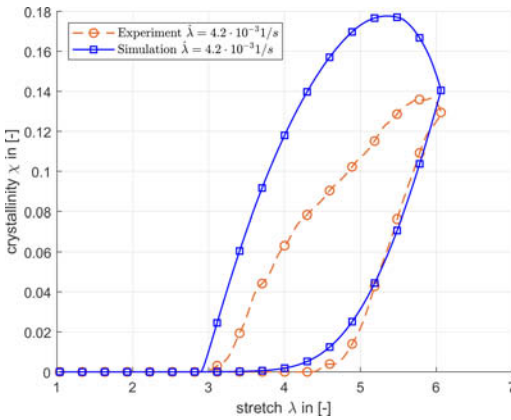

Figure 9. Crystallinity over stretch of unfilled natural rubber, simulation vs. experiment at low strainrate, experimental data from Candau (2014).

Table 1. Selected parameters used for the simulation shown in the Figures 8 & 9.

parameter	value	unit
crystallinity evolution		
x_0	0.4	–
M	0.0074	kg/mol
β	$1.5838 \cdot 10^{-10}$	–
empirical exponents		
m	2.05	–
n	1.28	–

crystallisation which depends on the difference of both strain energies rather than stresses, see equation (25).

With this evolution equation of crystallinity, the modelling of the stress-stretch response after uniaxial stretching shows promising results, shown in Figure 8 and Figure 9. Selected parameters of the model are listed in Table 1.

3 CONCLUSION

A thermomechanical approach to model strain induced crystallisation was presented, which distinguishes between three different phases in the specimen: crystallisable amorphous phase, the non-crystallisable amorphous phase and the crystalline phase. The total free energy contains free energies of the individual phases as well as a term of mixing entropy which is derived in detail. The concept was used to model crystallinity evolution at high stretched of rubbery elastomers. Please note further publications of the current author for more information on the presented study, 2017, 2019 and 2019.

REFERENCES

Candau, N. (2014). *Compréhension des mécanismes de cristallisation sous tension des élastomères en conditions quasi-statiques et dynamiques*. Ph. D. thesis.

Guilie, J., T.-N. Le, & P. Le Tallec (2015). Micro-sphere model for strain-induced crystallisation and three-dimensional applications. *Journal of the Mechanics and Physics of Solids 81*, 58–74.

Kaliske, M. & G. Heinrich (1999). An extended tube-model for rubber elasticity: statistical-mechanical theory and finite element implementation. *Rubber Chemistry and Technology 72*(4), 602–632.

Katz, J. R. (1925). Roentgenspektrogramme von Kautschuk bei verschiedenen Dehnungsgraden. Eine neue Untersuchungsmethode fuer Kautschuk und seine Dehnbarkeit. *Chem. ztg 49*, 353.

Lion, A., B. Dippel, & C. Liebl (2014). Thermomechanical material modelling based on a hybrid free energy density depending on pressure, isochoric deformation and temperature. *International Journal of Solids and Structures 51*(3-4), 729–739.

Loos, K., M. Johlitz, A. Lion, L. Palgen, & J. Calipel (2017). New ideas to represent strain induced crystallisation of elastomers. *Constitutive Models for Rubber X*.

Loos, K., A. Lion, M. Johlitz, A. Aydogdo, & J. Calipel (2019). Constitutive Modelling of Strain-Induced Crystallisation in Rubber. In *Constitutive Models for Rubber XI*.

Loos, K., A. Lion, M. Johlitz, & J. Calipel (2019). Strain-Induced Crystallisation in Natural Rubber: A new Modelling Approach.

Müller, I. (1973). *Thermodynamik, Die Grundlagen der Materialtheorie*. Bertelsmann Universitaetsverlag Duesseldorf.

Müller, I. (2013). *Grundzuege der Thermodynamik: mit historischen Anmerkungen*. Springer-Verlag.

Treloar, L. (1943). The elasticity of a network of long-chain molecules. {I}. *T. Faraday Soc. 39*, 36–41.

Williams, M. L., R. F. Landel, & J. D. Ferry (1955). The Temperature Dependence of Relaxation Mechanisms in Amorphous Polymers and Other Glass-forming Liquids. *J. Am. Chem. Soc. 77*(14), 3701–3707.